Magnetic Domain Confinement by Anisotropy Modulation

S. P. Li, W. S. Lew, J. A. C. Bland,* L. Lopez-Diaz, and C. A. F. Vaz
Cavendish Laboratory, University of Cambridge, Madingley Road, Cambridge CB3 0HE, United Kingdom

M. Natali and Y. Chen
Laboratoire de Microstructures et de Microélectronique (CNRS), 196 Avenue Henri Ravera, 92225 Bagneux Cedex, France
(Received 11 June 2001; published 11 February 2002)

The spin configuration in a magnet is in general a "natural" consequence of both the intrinsic properties of the material and the sample dimensions. We demonstrate that this limitation can be overcome in a homogeneous ferromagnetic film by engineering an anisotropy contrast. Substrates with laterally modulated single-crystal and polycrystalline surface regions were used to induce selective epitaxial growth of a ferromagnetic Ni film. The resulting spatially varying magnetic anisotropy leads to regular perpendicular and in-plane magnetic domains, separated by a new type of magnetic wall—the "anisotropy constrained" magnetic wall.

DOI: 10.1103/PhysRevLett.88.087202 PACS numbers: 75.70.Ak, 75.30.Kz, 75.60.Ej, 78.20.Ls

The size dependence of the spin configurations and reversal processes of magnetic nanostructures produced by lithographic patterning of thin magnetic films are of increasing interest [1]. While isolated "island" magnetic structures such as dots [2], wires [3], and other special geometries [4] have already been extensively studied, the experimental realization of patterned magnetic structures in a *chemically homogeneous* film remains an important goal. Generally the spin configurations in a magnet are defined by *both* the intrinsic properties of the material and the sample dimensions. Overcoming this limitation so that the local spin configurations in continuous films can be artificially controlled can open up new avenues for fundamental studies and device applications. First, such structures can be used as a planar patterned magnetic medium [5,6] without breaking the homogeneity of the magnetic film, which is important for avoiding reduced Curie temperature effects [7]. More importantly, it introduces a new way of controlling spin configurations instead of stabilizing the natural domains [8]. Furthermore, such locally controlled spin configurations do not have lateral dimension limitations and thus provide a reproducible switching mechanism, unlike geometrically restricted domains [9]. From a fundamental viewpoint, a film comprising regularly arranged regions with different magnetic anisotropy strengths, for instance, constitutes a multimagnetic phase system which would allow the study of magnetic dipolar and exchange interactions, wall formation, and domain wall resistance in highly controlled geometries.

In this Letter, we demonstrate an approach to controlling the magnetic structure in chemically homogeneous films via the artificial modification of substrate surface properties prior to growth. A modulated single/polycrystalline substrate surface is used to locally modify the magnetic anisotropy in the subsequently deposited magnetic films, which induces the desired magnetic structure. Selective epitaxial growth introduces an alternation between single-crystal and polycrystalline structures in the film, according to the substrate patterning (Fig. 1A). We chose the well-studied epitaxial Cu/Ni/Cu(001) structure to obtain an out-of-plane anisotropy. An epitaxial Ni(001) film with appropriate thickness shows perpendicular magnetic anisotropy (PMA) which is attributed to the magnetoelastic interaction induced by the Ni/Cu(001) interface [10]. In contrast, the magnetization of polycrystalline Ni lies in the film plane due to the dominant

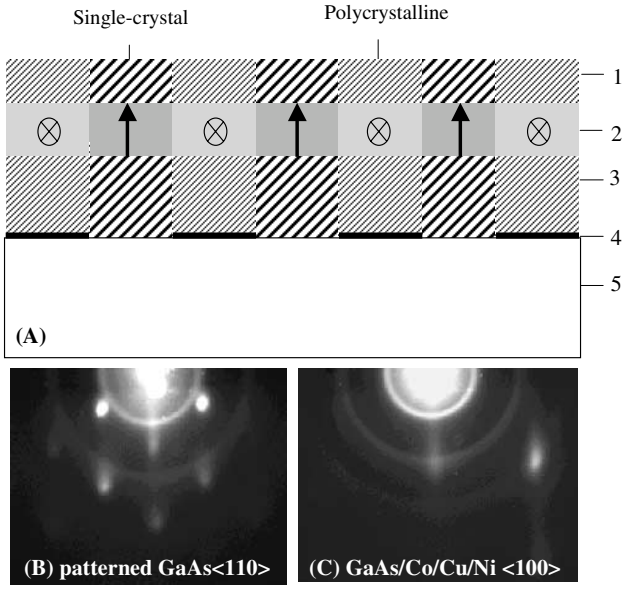

FIG. 1. A schematic of the selective epitaxial growth of a Ni(001) film (A). 1. Capping layer (Cu); 2. Magnetic film (Ni); 3. Buffer layer (Cu); 4. Ultrathin pattern (NiO); 5. Substrate (GaAs). Ultrathin NiO was used for the embedded pattern on a GaAs(001) substrate. A 1.8-nm-thick Co was used as a seed layer (not shown) to promote epitaxial growth on GaAs. The 70-nm-thick Cu buffer layer is thick enough to prevent the Co seed layer signal from being detected in the MOKE measurements. RHEED images taken from the patterned GaAs⟨110⟩ substrate (B) and the Ni⟨100⟩ film (C). The diffraction circles and dot pattern reveals the coexistence of the polycrystalline and epitaxial regions in the films.

demagnetizing field. The substrates that we used are GaAs(001) and two types of pattern were chosen: a 2-μm width with 4-μm-separation wire array, and a 7×7-μm^2 area with 3-μm-separation square dot array. Wire and dot arrays were obtained by optical lithography and a subsequent lift-off of 1-nm-thick Ni [11]. The ultrathin Ni patterns were then oxidized in air to become ultrathin NiO patterns. The patterned substrates were annealed at 500 °C for 2 h before film growth at room temperature. Continuous films of Cu(5 nm)/Ni(5 nm)/Cu(70 nm)/Co(1.8 nm) were deposited onto the substrates in an ultrahigh vacuum system (10^{-10} mbar) using molecular beam epitaxy (MBE) techniques. The 1.8-nm-thick Co is used as a seed layer to promote epitaxial growth on the GaAs substrate [12]. A thickness of 5 nm is selected for the Ni layer in order to obtain a strong PMA [10] and the 5-nm-thick Cu overlayer is used to prevent oxidation. While the films grown on the ultrathin NiO patterns are polycrystalline, those grown directly onto the GaAs surface are single crystal films. The results have been confirmed by *in situ* reflection high-energy electron diffraction (RHEED) analyses (Figs. 1B and 1C). *Ex situ* atomic force microscopy (AFM) was used to examine the sample surface, yielding statistical roughness parameters in the range similar to that of epitaxial continuous Cu/Ni/Cu films [10].

We carried out magneto-optical Kerr effect (MOKE) measurements at room temperature both in field-perpendicular-to-sample-film (polar) and field-parallel-to-sample-film (in-plane) geometries. The incidence angle of the laser in the polar and in-plane MOKE configurations was $\sim 0°$ and 35°, respectively. Spatially averaged MOKE signals are obtained from the patterned sample as the laser beam spot size was ~ 1 mm. Figure 2 shows typical hysteresis loops measured from the samples. Loop (A) is a polar MOKE curve obtained from an unpatterned epitaxial reference sample. The perfectly square hysteresis behavior with high remanence indicates a strong PMA in the epitaxial structure [13]. The measured in-plane MOKE loop from the wire sample is shown in (B). The magnetic field was applied along the wire direction during the measurement and the hysteresis loop reveals the magnetization process in the sample. The switching at the field ~ 100 Oe is due to the reversal of the in-plane magnetization in the polycrystalline regions. The sharp switch indicates that the reversal mechanism is controlled by domain nucleation and subsequent wall propagation. When the field is further increased towards saturation, the perpendicular magnetization in the epitaxial regions tends to align along the in-plane field direction through a magnetization rotation process, as evidenced by the high saturation field. The irreversible behavior near high field seen in the loop is due to the sensitivity of the in-plane MOKE geometry to the perpendicular component of the magnetization in epitaxial Ni [14]. A measurement that can respond only to the in-plane magnetization component can therefore be expected not to show such an irreversible feature, and this is confirmed by a superconducting quantum-interference device (SQUID) measurement [inset of loop (B)]. Loops (C) and (D) show the measured polar MOKE results from the wire and dot samples, respectively. In this measurement geometry only the perpendicular magnetization component can be detected. As the perpendicular field is reduced from positive saturation to zero, the magnetization in the polycrystalline Ni rotates back to the in-plane direction. However, the magnetization in the epitaxial Ni remains in the normal direction of the film. Upon increasing the field in the negative direction, the perpendicular magnetization switches to the reversed direction at its coercive field (~ 200 Oe) while the in-plane magnetization rotates progressively towards the out-of-plane direction in an increasing negative field. The polar MOKE loop obtained from the dot sample is squarer than that of the wire sample; this is because the area of the epitaxial Ni region in the dot sample is larger than that in the wire sample. The combined MOKE observations, supported by the sharp switch in low field and the gradual saturation seen in high field in both the in-plane and polar MOKE loops, clearly reveal the striking feature that *both* in-plane and out-of-plane magnetization coexist in the patterned samples.

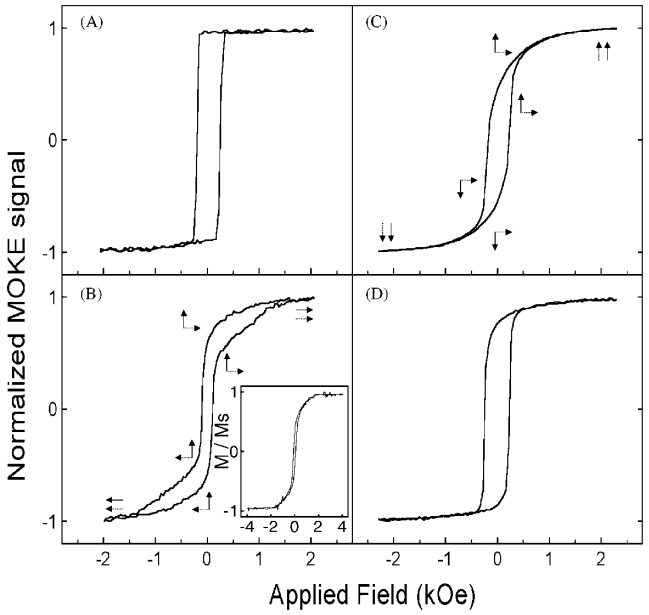

FIG. 2. MOKE hysteresis loops at room temperature. (A) A polar MOKE loop measured on the epitaxial Ni from an unpatterned reference sample. (B) In-plane MOKE loop taken from the wire sample, the inset shows the hysteresis loop measured by SQUID after subtracting the substrate signal. (C), (D) Polar MOKE loops measured on the wire and the dot samples, respectively. The solid (dotted) arrows show the magnetization orientations in the epitaxial (polycrystalline) Ni film. The magnetization orientations of the perpendicular Ni (up or down) in loop (B) and the in-plane Ni (right or left) in loop (C) is arbitrarily chosen.

The magnetic structures deduced from MOKE magnetometry were confirmed by magnetic force microscopy (MFM) imaging. In the MFM, the instrument was equipped with a CoCr coated Si tip, magnetized along the tip axis. During scanning, the magnetic tip oscillated at a chosen lift scan height while picking up the magnetic signal from the samples. Figures 3A and 3B show the MFM images of the dot and wire samples in the remanent state after saturating with a perpendicular field. A 100-nm lift scan height was used in these scans. The bright stripes in the images correspond to the out-of-plane Ni magnetization which has a strong magnetic signal and yields more contrast compared to the in-plane magnetization. To explore the reversal mechanism of the perpendicularly magnetized Ni we carried out MFM observations under a lower lift scan height. Figures 3C and 3D show the MFM images scanned at a 50-nm lift scan height for the dot and wire samples, respectively, in the remanent state obtained after perpendicular saturation. The lower lift scan height causes a stronger interaction between the emanating stray field from the tip and the samples. The dark regions in the out-of-plane Ni regions, encircled in white, are caused by the tip-induced switch. The high density of the reversed regions indicates a nucleation-dominated reversal process in our samples [15]. The reversal stages, including domain nucleation, local expansion from the nuclei, and widening by domain wall displacement, are completed in a very small external field interval as indicated by the rapid switch in the MOKE loops. To verify this we have repeated scanning in the center with a smaller scan area until the magnetization there has been almost fully switched (see the $\sim 20 \times 20\text{-}\mu\text{m}^2$ "cutoff" at the center of the images). The remaining unswitched hard magnetic entities near crystal defects, which define the final reversal stage, require higher magnetic fields to reverse.

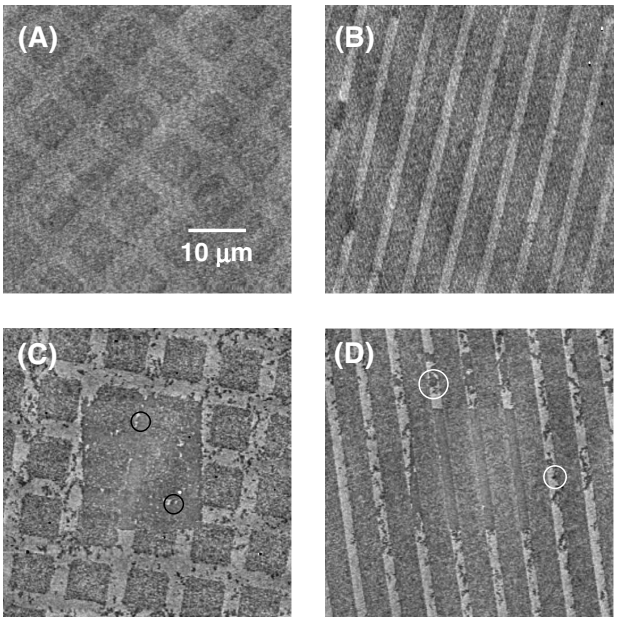

FIG. 3. MFM images in zero applied field after perpendicular magnetic field saturation. 100 nm (A), (B), and 50 nm (C), (D) lift scan height were used. For 50 nm lift scan height the magnetic stray field can induce switching in the perpendicularly magnetized Ni (the white circles mark the tip-induced switch in (D). In the center part of the image (C) and (D), the magnetization was almost fully switched by the repeated scans. The bright regions in the epitaxial Ni marked by black circles are the remaining unswitched hard magnetic entities after the repeated scans.

The 90° transition between the in-plane and out-of-plane regions is very sharp, as observed in Fig. 3. To our knowledge, a domain wall of this kind has not been studied before. Consequently, we have carried out micromagnetic numerical simulations in order to determine its width and internal structure. Using a conjugate gradient solver, the micromagnetic equilibrium equation was solved after saturating the sample along the perpendicular and in-plane directions. A cell size of 1 nm and typical Ni intrinsic parameters ($A = 9 \times 10^{-7}$ erg/cm, $M_s = 490$ emu/cm^3) were used in the simulation. $K_1 = 2.7 \times 10^6$ erg/cm^3 is the perpendicular anisotropy constant measured experimentally from Cu/Ni(5nm)/Cu(001) films [16]. The magnetization configuration in the transition region is represented in Fig. 4A. In Fig. 4B, we have plotted the variation of the out-of-plane component M_y along the z direction, where $z = 0$ corresponds to the boundary between the epitaxial (left) and polycrystalline (right) regions. A magnetic wall with the magnetization rotating in the plane of the wall ($M_z = 0$) can be found in Fig. 4A. In fact, the obtained wall is different in detail from the well-known Bloch wall and several new features can be observed. First, it is an asymmetric wall due to the different anisotropy strength on both sides of the boundary. Second, the wall is constricted in the film with no mobility under external perturbation. Finally, we note that immediately after the sharp transition there is a region with a small out-of-plane component ($M_y < 0$), which partially compensates the upwelling flux on the epitaxial region of the transition ($M_y > 0$). A similar effect is found in vortex cores [17]. By looking at Fig. 4B we see that the domain wall is approximately 15-nm wide. The dependence of wall width (δ_{DW}) on the anisotropy constant K_1 and the film thickness t is weak. A factor of 2 in the value of K_1 yields a variation in δ_{DW} of less than 5%, whereas a change of 1 nm in t gives 1% variation in δ_{DW}. The domain wall width sets a fundamental limit for the high pattern density achievable using the method described in this Letter. Additional simulations have been carried out by taking into account the finite size of the structures: it is found that the well-defined out-of-plane to in-plane transitions can be obtained for structures with a resolution down to 30 nm (Fig. 4C), which is quite promising for technological applications. Mathematically, the wall length can also be expressed by the contributions of two Bloch walls:

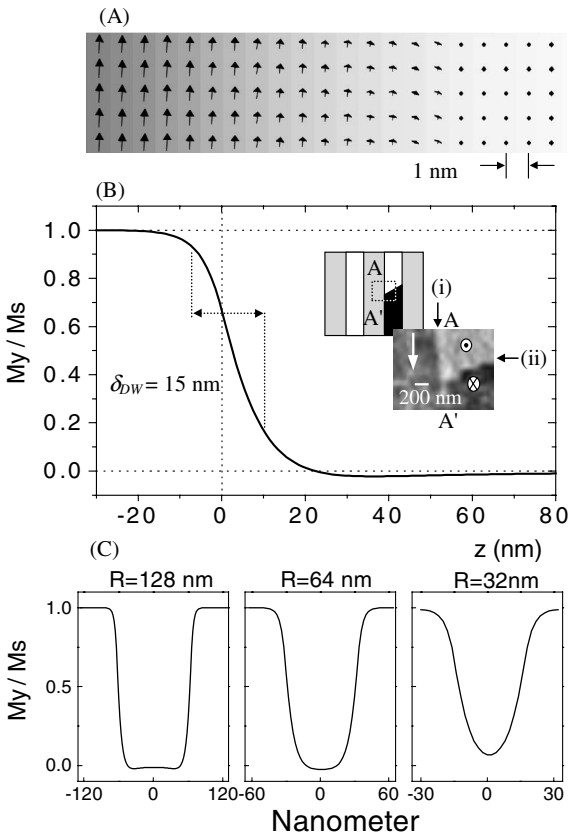

FIG. 4. (A) Computed magnetization configuration of the transition between the epitaxial and polycrystalline regions. (B) Variation of the perpendicular component of the normalized magnetization across the boundary ($z = 0$) between the perpendicular and in-plane magnetized Ni. Note the asymmetry of the wall due to the different magnetic anisotropy strengths of the in-plane and perpendicular Ni. The lower inset in (B) shows the zero field MFM image of the Ni striped sample (schematically shown in the upper inset) exhibiting (i) the new artificial 90° magnetic wall and (ii) the well-known 180° Bloch wall which is defined by the reversal of the perpendicularly magnetized Ni inside the epitaxial wire structure. The white arrow indicates the in-plane magnetization whereas the symbols ⊙, ⊗ refer to the direction of the perpendicular magnetization. (C) The calculated magnetization profiles for different periodicity of the Ni wire structure. The Resolution (R) is defined by the half period of the structure, where the origin is the center of the polycrystalline Ni wire, and a period is taken as two times the width of the polycrystalline Ni stripe.

$$\delta = \frac{\pi}{2}\left(\frac{1}{\sqrt{K_1 - 2\pi M_s^2}} + \frac{1}{\sqrt{2\pi M_s^2}}\right)\sqrt{A}. \qquad (1)$$

Equation (1) yields $\delta \sim 15.5$ nm for the same parameters given above, which agrees well with the numerically simulated result.

In conclusion, we have created modulated magnetic structures in chemically homogeneous Ni films by inducing a spatially varying magnetic anisotropy via selective epitaxy. A new type of magnetic wall has been observed which we term the "anisotropy constrained" magnetic wall. The wall structure differs from that of naturally occurring domain walls, e.g., the Néel and Bloch walls [18] or the geometrically restricted wall [19]. We conjecture that for other thin film systems with perpendicular anisotropy, such as Co/Au [20], Fe/Ag [21], etc., similar results could also be realized and that this could be extended to antiferromagnetic systems (in this case by selective interface exchange coupling). Finally, our simulations indicate that the modulated structures can be defined at the deep submicron scale.

This research was supported by the EC, ESPRIT program (MASSDOTS Project No. 22464). We acknowledge the assistance of J. D. Mackenzie and P. K. H. Ho. W. S. L. thanks the Cambridge Commonwealth Trust for support. C. A. F. V. is supported by Programa PRAXIS XXI (Portugal).

*To whom correspondence should be addressed.
Email address: jacb1@phy.cam.ac.uk

[1] R. P. Cowburn *et al.,* Phys. Rev. Lett. **83**, 1042 (1999); E. Gu *et al.,* Phys. Rev. Lett. **78**, 1158 (1997).
[2] M. Hehn *et al.,* Science **272**, 1782 (1996); O. Fruchart *et al.,* Phys. Rev. Lett. **82**, 1305 (1999).
[3] C. Mathieu *et al.,* Phys. Rev. Lett. **81**, 3968 (1998); A. O. Adeyeye *et al.,* Appl. Phys. Lett. **70**, 1046 (1997).
[4] S. P. Li *et al.,* Phys. Rev. Lett. **86**, 1102 (2001).
[5] C. Chappert *et al.,* Science **280**, 1919 (1998).
[6] B. D. Terris *et al.,* Appl. Phys. Lett. **75**, 403 (1999); G. J. Kusinski *et al.,* Appl. Phys. Lett. **79**, 2211 (2001); D. Weller *et al.,* J. Appl. Phys. **87**, 5768 (2000).
[7] R. P. Cowburn *et al.,* Appl. Phys. Lett. **70**, 2309 (1997).
[8] L. Krusin-Elbaum *et al.,* Nature (London) **410**, 444 (2001).
[9] T. Taniyama *et al.,* Phys. Rev. Lett. **82**, 2780 (1999); U. Ebels *et al.,* Phys. Rev. Lett. **84**, 983 (2000).
[10] W. L. O'Brien and B. P. Tonner, Phys. Rev. B **49**, 15 370 (1994); S. Hope *et al.,* Phys. Rev. B **55**, 11 422 (1997).
[11] 1 nm Ni is used for simplicity in this experiment. In principle, half a monolayer Ni is sufficient for the selective epitaxial growth.
[12] W. S. Lew *et al.,* J. Appl. Phys. **87**, 5947 (2000).
[13] C. A. F. Vaz and J. A. C. Bland, Phys. Rev. B **61**, 3098 (2000).
[14] J. Lee, G. Lauhoff, and J. A. C. Bland, Phys. Rev. B **56**, R5728 (1997).
[15] J. Pommier *et al.,* Phys. Rev. Lett. **65**, 2054 (1990).
[16] G. Bochi *et al.,* Phys. Rev. B **53**, R1729 (1996).
[17] A. Hubert and R. Schäfer, *Magnetic Domains: The Analysis of Magnetic Microstructures* (Springer-Verlag, Berlin, 1998).
[18] F. Bloch, Z. Phys. **74**, 295 (1932); L. Néel, C. R. Acad. Sci. Paris **241**, 533 (1955).
[19] P. Bruno, Phys. Rev. Lett. **83**, 2425 (1999).
[20] R. Allenspach, M. Stampanoni, and A. Bischof, Phys. Rev. B **65**, 3344 (1990).
[21] Z. Q. Qiu, J. Pearson, and S. D. Bader, Phys. Rev. Lett. **70**, 1006 (1993).